

A Helix in Helices: A Helical Conjugated Polymer That Has Helically Arranged Hydrogen-Bond Strands

Ryoji Nomura, Junichi Tabei, Shino Nishiura, and Toshio Masuda*

Department of Polymer Chemistry, Graduate School of Engineering, Kyoto University, Kyoto 606-8501, Japan

Received August 8, 2002; Revised Manuscript Received November 19, 2002

ABSTRACT: The secondary structure of Rh-based stereoregular *cis*-poly(*N*-propargylamides) was proposed on the basis of the UV–vis, CD, and IR spectra, the wormlike touched-bead model theory, and a semiempirical molecular orbital calculation. The IR spectra demonstrated the formation of well-ordered intramolecular hydrogen bonding between the pendant amide groups. The relatively red-shifted absorption and the intense CD effects indicate that the main chain twists only slightly from coplanarity to exist in a helical conformation with a large helix pitch. Analyzing the intrinsic viscosity of a polymer, (\pm)-poly(*N*-propargyl-2-ethylhexanamide), on the basis of the wormlike touched-bead model theory, showed a large helix pitch per monomer unit (h , 0.2 nm), which also supports the above characteristics that the main chain loosely twists. A semiempirical calculation with the AM1 method showed that the helical conjugated backbone is surrounded by two helically arranged hydrogen-bond strands.

Introduction

α -Helix is one of the most fundamental secondary conformations of proteins.¹ Each n th peptide unit hydrogen-bonds with the $(n + 4)$ th one, and all amide groups are joined with hydrogen bonds. This well-ordered hydrogen bonding significantly contributes to stabilization of the α -helical conformation. It is unfortunate, however, that orderly arrangement of hydrogen bonding in synthetic polymers is quite difficult. Although many attempts have been made on this issue,^{2,3} successful results were only recently obtained by Nolte et al. and by us, independently. Nolte and co-workers synthesized poly(isocyanides) having oligopeptide pendants.⁴ The preference of the side chain to form a β -sheetlike structure works as a driving force to twist the main chain into a helical conformation. The IR data suggest that the hydrogen bonds are well-arranged and located intramolecularly. We introduced amide groups to polyacetylene and succeeded in constructing an ordered hydrogen bonding.⁵ Specifically, the pendant amide groups in stereoregular (*cis*) poly(*N*-propargyl-alkylamides), poly(**1**) (Chart 1), intramolecularly hydrogen-bond, which simultaneously rigidifies the polymer backbone. Polymers from monosubstituted acetylenes, unless they have very bulky substituents, are generally flexible, except for stereoregular *cis*-poly(propionic esters), $[\text{CH}=\text{C}(\text{CO}_2\text{R})]_n$, so that they cannot adopt a helical conformation.^{7,8} However, the backbone rigidity of poly(**1**), enhanced by the hydrogen bond, enables the main chain to take a helical structure with a large helical domain size.

In this paper, we show the secondary structure of poly(*N*-propargylamide) that is predicted on the basis of UV–vis, CD, and IR spectra, the wormlike–chain wormlike touched-bead model theory,⁹ and the semiempirical molecular orbital calculation. We found that the conjugated main chain of poly(*N*-propargylamide) loosely twists to form a helical conformation which is

surrounded by two helically arranged hydrogen-bond strands as schematically illustrated in Chart 1.

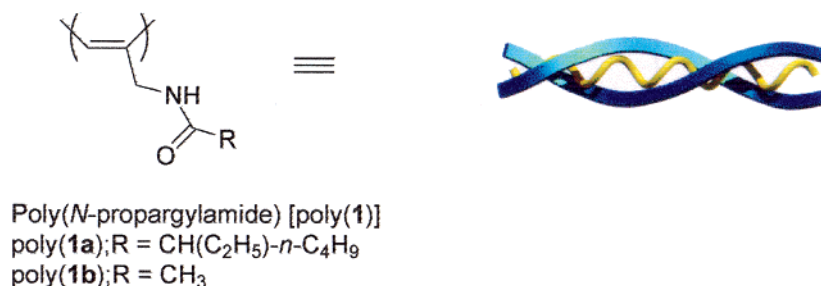
Results and Discussion

UV–vis spectroscopy is a convenient indication for the degree of the main chain conjugation. The degree of main chain conjugation of substituted polyacetylenes strongly depends on the geometrical structure of the double bond and on the side chain structure.⁷ The geometrical structure (*cis* or *trans*) can be controlled by catalysts. For instance, Rh catalysts are quite effective to give good yields of polymers with excellent *cis* stereoregularity.^{7,10} On the other hand, W-based *trans*-rich polymers possess *trans*-rich structures, which leads to a large degree of main chain conjugation compared with Rh-, Fe-, and Mo-based *cis* or *cis*-rich polymers.¹¹ Regarding the influence of the side chain structure, aromatic rings conjugatively connected with the main chain double bonds enhance the degree of the main chain conjugation,^{7,11} while polymers from aliphatic monosubstituted acetylenes are less conjugated.¹² Hence, *cis* polymers from aliphatic monosubstituted acetylenes, prepared with Rh catalysts, possess the lowest level of main chain conjugation among the acetylenic polymers, which relates to the fact that the cutoff wavelength of most *cis* aliphatic polymers appears below 420 nm.

However, Rh-based poly(*N*-propargylamides) display λ_{max} at 400 nm in CHCl_3 when they exist in the helical conformation.⁵ The cutoff wavelength reaches 480 nm. These results are in contrast to those of poly(propionic esters) which possess a tightly twisted helical main chain.¹³ Computational calculations have suggested that the dihedral angle around the single bond is 107° – 120° for poly(propionic esters).^{13b} Thus, the degree of main chain conjugation of poly(propionic esters) is quite low, which corresponds to the large band gap (cutoff wavelength = 400 nm). Therefore, the unexpectedly red-shifted absorption of poly(*N*-propargylamides) indicates that the main chain double bonds are well-conjugated. At least, it can be concluded that the averaged dihedral angle about the single bond is larger than 120° .

* Corresponding author: Tel +81-75-753-5613; Fax +81-75-753-5908; e-mail masuda@adv.polym.kyoto-u.ac.jp.

Chart 1



CD spectra of poly(*N*-propargylamides) with chiral side chains display very intense Cotton effects in the absorption region of the main chain.⁵ Concentration independence of the chiroptical properties, including the Cotton effects and optical rotation, reveals that the chirality originates from the helical conformation of the individual polymer main chain. From the UV and CD data, it can be concluded that the main chain loosely twists from the coplanar conformation to adopt a helical one.

IR spectra of poly(*N*-propargylamides) have clearly demonstrated that the N–H and carbonyl groups are hydrogen-bonded.⁵ Because the peaks originating from partially hydrogen-bonded or non-hydrogen-bonded amide groups have not been observed in the IR spectra, all amide groups participate in the hydrogen bonding. These IR bands are independent of concentration, meaning that the hydrogen bonds are constructed intramolecularly. This hydrogen bonding rigidifies the polymer backbone and promotes the self-organization of the main chain into the helical conformation. Therefore, the carbonyl oxygen and proton on nitrogen, which are hydrogen-bonded to each other, should be located in the distance between 2.6 and 3.0 Å.

The **wormlike touched-bead model theory** is next applied to a sample of (±)-poly(*N*-propargyl-2-ethylhexanamide) [poly(**1a**)] to estimate the pitch *h* of the helix. According to the theory,⁹ the intrinsic viscosity $[\eta]$ can be predicted as a function of the molar mass M_L per unit contour length, the polymer molecular weight *M*, the persistence length *q*, and the diameter of the bead *d_b*. Thus, the relationship between the $[\eta]$ and *M* gives *q*, *d_b*, and M_L , and the last parameter eventually leads to *h*. The relation between $[\eta]$ and the weight-average molecular weight M_w , the so-called Hawnink–Mark–Sakurada plot, can be determined experimentally by gel permeation chromatography equipped with a refractive index detector, a light-scattering detector, and a viscometer using the universal calibration curve. The red curve in Figure 1 shows the experimental data of the Hawnink–Mark–Sakurada plot for the poly(**1a**) sample. A trial-and-error method was applied to find *q* and *d_b* values, resulting in the closest agreement between the theory and experimental $[\eta]$ as shown in the blue curve in Figure 1. The theory fits the experimental data most closely when *q*, *d_b*, and M_L are chosen to be 13.5 nm, 2.00 nm, and 905 nm^{−1}, respectively. From the M_L value, *h* is calculated to be 0.20 nm. Comparison of the *q* value with that of poly(4-carboxylphenylacetylene) (3.4 nm)¹³ clearly indicates that poly(*N*-propargylamides) possess a stiff main chain, while poly(4-carboxylphenylacetylene) belongs to the category of flexible chain. However, there is no significant difference in *h* value between these polymers [0.22 nm for the *h* of poly(4-carboxylphenylacetylene)].¹⁴ This means that the main

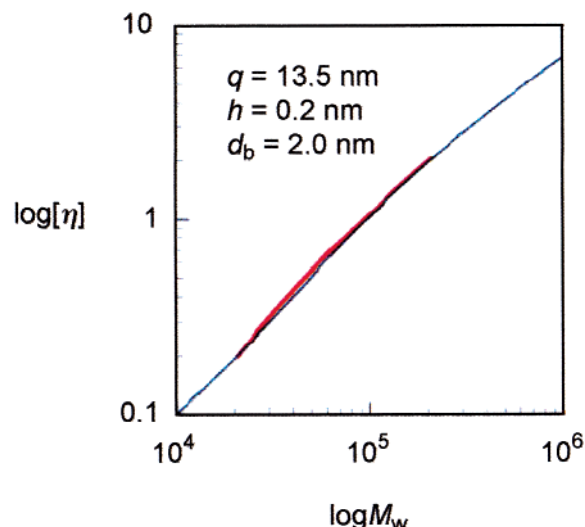


Figure 1. Molecular weight dependence of the intrinsic viscosity of the sample of poly(**1a**): red curve, experimental data; blue curve, theoretical values calculated by the wormlike touched-bead model theory.

chain conformation of poly(*N*-propargylamides) is similar to that of poly(4-carboxylphenylacetylene) except for the persistence length, i.e., rigidity of the backbone. The computational molecular mechanics calculations of cis–transoidal poly(phenylacetylene) have suggested that the dihedral angle of the single bond for the most stable conformation ranges between 147° and 155°. ^{8c} Thus, it is reasonably concluded that poly(*N*-propargylamides) have a relatively large dihedral angle as with poly(phenylacetylenes) having small ring substituents.

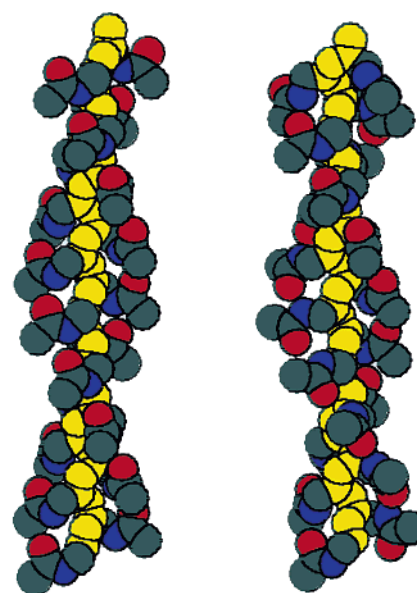
Molecular modeling using CPK molecular models gave two possible conformations for poly(*N*-propargylamides). One has a very tightly twisted main chain where the hydrogen bonds are formed between the *n*th and (*n* + 3)th repeating units. Hydrogen bonds are located between *n*th and (*n* + 2)th repeating units for the other model. The CPK molecular modeling study apparently ruled out any other conformations. Computational modeling suggested that the dihedral angle around single bonds must be below 120° for the former model. The above-described discussion based on the spectroscopic data and the wormlike model theory revealed that the main chain conformation is a loosely twisted helix and close to that of poly(phenylacetylenes). Thus, the former conformation can be ruled out, and the latter model is probable, in which the dihedral angle ranges between 120° and 160°.

The **semiempirical molecular orbital calculation** was finally carried out for geometrical. First, we prepared 20-mers of *N*-optimization of poly(*N*-propargylamide)–propargylethanamide (**1b**) as initial models, in which both end groups were terminated with hydrogen.

The dihedral angles around the double bonds were fixed at 180° , and those around the single bonds were varied from 120° to 160° by the step of 10° . The side chain conformation of the initial models was set in such a way to form hydrogen bonding between n th and $(n + 2)$ th pendant amide groups. All carbonyl double bonds were set to point in the same direction. The structural optimization was first carried out for these 20-mers by using the MM2 method. The MM2 geometrical optimization of an initial model with the dihedral angle of the single bond of 160° gave a right-handed helix where the dihedral angles, except for those of the terminal segments, range from 154° to 158° . The averaged dihedral angle was 153° for this model. The other initial models gave an alternative result. Specifically, the most stable structure that was obtained from the initial models with dihedral angles from 120° to 150° was also a right-handed helix, in which the averaged dihedral angles was between 141° and 145° . Further calculation was performed by using the AM1 method on these two 20-mers with the averaged dihedral angles of the single bond of 153° and 141° , respectively. These calculations provided the same results. Namely, both models were geometrically optimized into a 20-mer with the averaged dihedral angle of 139° .¹⁵

The computational simulation does not always provide the actual structure. However, as shown below, the computationally optimized conformation very reasonably explains the theoretically and experimentally obtained data. For example, the distance between the terminal carbons was 41 Å for the optimal 20-mer, which corresponds to the helix pitch per monomer unit h of 0.205 nm. This h value well agrees with that obtained by the wormlike touched-bead model theory (0.2 nm) as described above. When this conformation is applied to poly(**1a**), the diameter of the polymer is estimated to be approximately 20 Å. This value is also in good agreement with d_b (2.00 nm) which roughly corresponds to the polymer diameter. The distance between the nitrogen at an n th unit and the carbonyl oxygen at the corresponding $(n + 2)$ th one (3.0 ± 0.08 Å) in the optimized conformation means the formation of a hydrogen bond between these repeating units, which can explain the experimental IR data. Therefore, we assume that the present optimized structure is quite close to the actual one.¹⁶

The optimized structure of the 20-mer is illustrated in Figure 2a. The main chain is a right-handed helix but only loosely twists from coplanarity. This result contrasts with the tightly twisted helical poly(propionic esters).^{13b} Interestingly, the side chain amide groups are aligned and accumulated along the helix axis. The side chain amide groups form two helical hydrogen-bond strands surrounding the helical conjugated backbone. Each hydrogen-bond strand has approximately 10 amide groups per turn. In this model, termed the parallel form, all amide groups point to the same orientation along the helical axis, and thus, the polymer should have a very large dipole moment like the α -helices. The computationally estimated dipole moment of the parallel form by using the MOS-F method was as large as 113 D and directs toward the helical axis. This is simply because all amide groups in the initial model were set to orient in the same direction. However, it is more probable that the two hydrogen-bond strands direct in opposite directions to each other as shown in the antiparallel form (Figure 2b). Indeed,



(a) Parallel Form (b) Antiparallel Form

Figure 2. Computationally optimized structure of 20-mer of *N*-propargylethanamide (**1b**) terminated by hydrogen: (a) parallel form; (b) antiparallel form.

the antiparallel form is the most stable conformation when the direction of the amide groups was alternatively changed in the initial model. The antiparallel form has a similar conformation to that of the parallel form; the averaged dihedral angle about the single bond was 132° . In this form, the dipole moment was as small as 12 D. The simulation indicated that the antiparallel form is more stable than the parallel form by approximately 1 kcal/mol per monomer unit. Although direct comparison of the heat of formation of these two models may be inappropriate, we assume that the antiparallel form is more plausible.

Conclusion

In the present study, we demonstrated the secondary structure of poly(*N*-propargylamides) using various spectroscopies, the wormlike touched-bead model theory, and the computational molecular orbital calculation. The computationally optimized structure well explained the data theoretically and experimentally obtained. The main chain double bond loosely twisted from coplanarity to exist in a loose helix with a large helix pitch. Two helically arranged hydrogen-bond strands surround the helical backbone.

In α -helical peptides, the large dipole moment directing the helix axis significantly participates in their functions such as electron transporting, molecular recognition, and so on.¹⁷ If the parallel form can be selectively generated, poly(*N*-propargylamides) would possess a very large dipole moment like the α -helices. Furthermore, poly(*N*-propargylamides) theoretically supply three pathways for electron transfer: the conjugated main chain and the two hydrogen bond strands. Thus, they can be regarded as a molecular wire for electron transfer. Unfortunately, the dipole along the helical axis is probably quite small because the antiparallel form is likely to be favorable. However, we believe that alignment of the dipole is possible by introducing appropriate end groups that work only as a hydrogen-bonding donor or acceptor. We are currently investigat-

ing this matter by applying the Rh-catalyzed living polymerization technique.

Experimental Section

General. The molecular weights and polydispersities of the polymers were determined by using gel permeation chromatography (eluent, chloroform; Shodex columns K804, K805, and K806; calibrated by polystyrene standards). ^1H NMR spectra were recorded with a JEOL EX-400 spectrometer. CD, UV-vis, and IR data were obtained using a Jasco J800 spectropolarimeter, a Jasco V-550 spectrophotometer, and a Shimadzu FTIR-8100 spectrophotometer, respectively. The refractive index increment, $\partial n/\partial c$, was determined using an Otsuka Electronics DRM-1020 differential refractometer. Melting points were measured on a Yanaco micro-melting point apparatus and were not corrected. CHCl_3 was distilled from P_2O_5 under nitrogen. Et_3N was distilled over CaH_2 .

Synthesis of (\pm)-*N*-Propargyl-2-ethylhexanamide (1a**).** Commercially available (\pm)-2-ethylhexanoic acid was converted into the corresponding acyl chloride with thionyl chloride, which was followed by the reaction with *N*-propargylamine in the presence of pyridine. Purification was carried out by SiO_2 column chromatography, followed by recrystallization with hexane; mp 49 °C. ^1H NMR (CDCl_3 , 400 MHz): δ 0.88 (m, 6H), 1.27 (m, 4H), 1.46 (m, 2H), 1.61 (m, 2H), 2.00 (p, 1H, $J = 4.8$ Hz), 2.23 (s, 1H), 4.07 (d, 2H, $J = 2.4$ Hz), 6.04 (s, 1H). ^{13}C NMR (CDCl_3 , 100 MHz): δ 11.9, 13.9, 22.7, 26.0, 28.8, 29.7, 32.4, 49.3, 71.2, 79.8, 175.7. IR (KBr): 3306, 2961, 1655, 1546, 1238, 662 cm^{-1} . Anal. Calcd for $\text{C}_{11}\text{H}_{19}\text{NO}_2$: C, 72.90; H, 10.50; N, 7.73. Found: C, 72.81; H, 10.22; N, 7.73.

Polymerization. The polymerization was carried out by using $[(\text{nbd})\text{RhCl}]_2$ as a catalyst and Et_3N as a cocatalyst in distilled CHCl_3 under the following conditions; $[\mathbf{1a}] = 0.50$ M, $[\text{Cat}] = [\text{Cocat}] = 5.0$ mM, 1 h, 30 °C. A solution of $[(\text{nbd})\text{RhCl}]_2$ and Et_3N in distilled CHCl_3 was added to a solution of **1a** in CHCl_3 at 30 °C. The solution was poured into methanol to precipitate the polymers. The resultant polymers were collected, filtered, and dried under reduced pressure to isolate poly(**1a**) as a yellow powder in 61% yield. The cis stereoregularity was confirmed to be quantitative by ^1H NMR. The M_n and M_w estimated by GPC (eluent CHCl_3 , polystyrene standards) were 18 000 and 43 000, respectively.

Hauwink–Mark–Sakurada Plot. The data used in the wormlike touched-bead model, that is, molecular weight dependence of the intrinsic viscosity, were obtained using a GPC system equipped with an RI detector (Jasco RI-930 Model), a viscometer, a light-scattering detector (Viscotek T60A Model), and a Shodex column K804 (eluent, CHCl_3). The refractive index and the relative viscosity η_r of the eluate were simultaneously recorded with this apparatus. The former quantity was converted to the mass concentration c of the eluted polymer by using the refractive index increment $\partial n/\partial c$ of the polymer. $[\eta]$ was approximately evaluated by dividing η_r^{-1} by c . The M_w of the eluted polymer was estimated on the assumption that the hydrodynamic volume of the copolymer, defined by $[\eta]M_w$, is given by the universal function of elution time.

Computational Calculation. Semiempirical calculations were performed using the MOPAC 2000 developed by Fujitsu and Dr. J. J. P. Stewart. The used semiempirical Hamiltonian was AM1 with EF algorithms. The initial models were constructed with CS ChemBats3D Pro (version 5.0, Cambridge Soft Corp.). MM2 calculations were carried out by using CS Chem3D Pro.

Acknowledgment. The authors thank Assistant Professor T. Sato at Osaka University for the data analyses and Assistant Professor M. Kamigaito and Professor M. Sawamoto for the measurement of the refractive index increment. Thanks are also due to Professor T. Yoshizaki for his valuable suggestions and reviewing the manuscript. This work was supported by

a Grant-in-Aid for Scientific Research from Japan Society for the Promotion of Science.

References and Notes

- (1) (a) Schulz, G. E.; Schirmer, R. H. *Principles of Protein Structure*; Springer-Verlag: New York, 1979. (b) Branden, C.; Tooze, J. *Introduction to Protein Structure*, 2nd ed.; Newion Press: New York, 1999.
- (2) (a) Nakahira, T.; Lin, F.; Boon, C. T.; Karato, T.; Annaka, M.; Yoshikuni, M.; Iwabuchi, S. *Polym. J.* **1997**, *29*, 701–704. (b) Nakahira, T.; Fan, L.; Boon, C. T.; Fukada, Y.; Karato, T.; Annaka, M.; Yoshikuni, M. *Polym. J.* **1998**, *30*, 910–914.
- (3) (a) Li, B. S.; Cheuk, K. K. L.; Salhi, F.; Lam, J. W. Y.; Cha, J. A. K.; Xiao, X.; Bai, C.; Tang, B. Z. *Nano Lett.* **2001**, *1*, 323–328. (b) Tang, B. Z. *Polym. News* **2001**, *26*, 262–272 and references therein.
- (4) Cornelissen, J. J. L. M.; Donners, J. J. J. M.; de Gelder, R.; Graswinckel, W. S.; Metselaar, G. A.; Rowan, A. E.; Sommerdijk, N. A. J. M.; Nolte, R. J. M. *Science* **2001**, *293*, 676–680.
- (5) (a) Nomura, R.; Tabei, J.; Masuda, T. *J. Am. Chem. Soc.* **2001**, *123*, 8430–8431. (b) Nomura, R.; Tabei, J.; Masuda, T. *Macromolecules* **2002**, *35*, 2955–2961. (c) Tabei, J.; Nomura, R.; Masuda, T. *Macromolecules* **2002**, *35*, 5405–5409.
- (6) Nomura, R.; Fukushima, Y.; Nakako, H.; Masuda, T. *J. Am. Chem. Soc.* **2000**, *122*, 8830–8836.
- (7) For general reviews of substituted polyacetylenes, see: (a) Masuda, T. In *Catalysis in Precision Polymerization*; Kobayashi, S., Ed.; Wiley: Chichester, 1997; Chapter 2.4. (b) Masuda, T. In *Polymeric Material Encyclopedia*; Salamone, J. C., Ed.; CRC: New York, 1996, Vol. 1, pp 32–39.
- (8) (a) Ciardelli, F.; Lanzillo, S.; Pieroni, O. *Macromolecules* **1974**, *7*, 174–179. (b) Aoki, T.; Kokai, M.; Shinohara, K.; Oikawa, E. *Chem. Lett.* **1993**, 2009–2012. (c) Yashima, E.; Huang, S.; Matsushima, T.; Okamoto, Y. *Macromolecules* **1995**, *28*, 4184–4193.
- (9) Yamakawa, H. *Helical Wormlike Chains in Polymer Solutions*; Springer: Berlin, 1997.
- (10) Tabata, M.; Sone, T.; Sadahiro, Y. *Macromol. Chem. Phys.* **1999**, *200*, 265–282.
- (11) Masuda, T.; Karim, S. M. A.; Nomura, R. *J. Mol. Catal. A: Chem.* **2000**, *160*, 125–131.
- (12) For example: (a) Leclerc, M.; Prud'honune, R. E. *J. Polym. Sci., Polym. Phys. Ed.* **1985**, *23*, 2021–2030. (b) Tsuchihara, K.; Masuda, T.; Higashimura, T. *Polym. Bull. (Berlin)* **1988**, *20*, 343–348.
- (13) (a) Nakako, H.; Mayahara, Y.; Nomura, R.; Tabata, M.; Masuda, T. *Macromolecules* **2000**, *33*, 3978–3982. (b) Nakako, H.; Nomura, R.; Masuda, T. *Macromolecules* **2001**, *34*, 1496–1502.
- (14) Ashida, Y.; Sato, T.; Morino, K.; Maeda, K.; Yashima, E.; Okamoto, Y. *J. Jasco Rep.* **2001**, *43*, 33–36.
- (15) Computational optimization of initial models with dihedral angle less than 120° also gave helical conformation where individual n th amide group is located most closely to the $(n + 3)$ th one. However, the distance of the oxygen and nitrogen atoms exceeded 4 Å, which ruled out the possibility of hydrogen bonding between the n th and $(n + 3)$ th repeating units.
- (16) The mechanism of the solvatochromism and thermochromism of poly(*N*-propargylamides), which originate from the conformational change between the helical and disordered states,^{5b} is now clearly explained. In the helical state, the backbone has very large persistence length h ; thus, the order of the main-chain conjugation is quite expanded. On the other hand, the polymers prefer a random conformation when the hydrogen bonding collapses. Consequently, the main chain conjugation is frequently cleaved at the point where the dihedral angle is small, which contributes to the large band gap, blue-shifted cutoff wavelength, and achromatic solution.
- (17) Hol, W. G. J.; van Duijnen, P. T.; Berendsen, H. J. C. *Nature (London)* **1978**, *273*, 443–446.